Arch Virol (2008) 153:1575–1579
DOI 10.1007/s00705-008-0143-5

BRIEF REPORT

A mutational shift from domain III to II in the internal ribosome entry site of hepatitis C virus after interferon–ribavirin therapy

Kei Ogata · Takahito Kashiwagi · Jun Iwahashi · Koyu Hara · Haruhito Honda · Tatsuya Ide · Ryukichi Kumashiro · Michinori Kohara · Michio Sata · Hiroshi Watanabe · Nobuyuki Hamada

Received: 7 August 2007 / Accepted: 21 May 2008 / Published online: 1 July 2008

Abstract We focused on the relationship between variation in the IRES of hepatitis C virus (HCV) genotype 1b and clinical outcome, since the internal ribosome entry site (IRES) has a comparatively low heterogeneity and it might be easy to find unique substitutions. Patients infected with HCV were selected using strict criteria, and unique mutations in the IRES were extracted by the subtraction of common mutations. We found that most mutations accumulated in domain III (dIII) of IRES in sustained virological responders (SVRs) and non-SVRs before therapy. However, these mutations were exclusively observed in domain II (dII) in non-SVR at 2 weeks after the start of therapy.

Hepatitis C virus (HCV) is an enveloped RNA virus of the genus *Hepacivirus* in the family *Flaviviridae* [2]. The genomic RNA is a plus strand consisting of approximately 9,600 nucleotides, which contains a large open reading frame and two untranslated regions. The untranslated regions (UTR) are present at each end of the genome (5′ and 3′ termini) and are involved in not only the translation of viral proteins but also genomic replication. An especially highly conserved region (about 341 nucleotides) in the 5′ UTR is known to act as an internal ribosome entry site (IRES), which is essential for the translation of viral proteins [17, 18]. The IRES forms a tertiary structure for ribosome binding and subsequent protein synthesis [4]. An artificial alteration of the sequence can severely affect translational activity [6].

HCV is a significant cause of morbidity and mortality, infecting over 170 million people worldwide. The majority (about 80%) of individuals with HCV infection develop chronic hepatitis, which can progressively lead to cirrhosis (10–20%), and eventually to hepatocellular carcinoma (5%). Despite recent efforts, the current therapy [pegylated-interferon (IFN) with ribavirin] for HCV infection remains inadequate for approximately half of all patients. The mechanisms of tolerance against this therapy are still unknown. HCV is genetically heterogeneous, and it circulates as a population of closely related genomes, referred to as quasispecies [12]. Previous studies have shown that specific regions in the HCV genome, such as the IRES and the NS5B coding region, accumulate nucleotide substitutions in patients receiving antiviral therapy [8, 16]. These results suggest that some mutants show tolerance against the current therapy. However, the significance of genetic variations in these regions is still not fully understood either biochemically or clinically. The quasispecies, which normally appear during treatment, consist of many heterogeneous clones. This heterogeneity makes the interpretation of the relationship between clinical outcome and resistance mutations difficult.

K. Ogata · T. Kashiwagi · J. Iwahashi · K. Hara · H. Honda · H. Watanabe · N. Hamada (✉)
Division of Infectious Diseases, Department of Infectious Medicine, Kurume University School of Medicine, 67 Asahi-machi, Kurume, Fukuoka 830-0011, Japan
e-mail: nhamada@med.kurume-u.ac.jp

K. Ogata · T. Ide · R. Kumashiro · M. Sata
Division of Gastroenterology, Department of Internal Medicine, Kurume University School of Medicine, 67 Asahi-machi, Kurume, Fukuoka 830-0011, Japan

M. Kohara
Department of Microbiology and Cell Biology, The Tokyo Metropolitan Institute of Medical Biology, 3-18-22 Honkomagome, Bunkyo-ku, Tokyo 113-8613, Japan

In this study, we examined the relationship between the IRES of HCV from the pre- and in-treatment sera of the patients (sustained virological responder (SVR) and non-SVR to IFN–ribavirin therapy) and its clinical outcome, because there is said to be a comparatively lower mutant spectrum complexity in the IRES in comparison to the coding region. Previous reports have suggested that no clinically significant variations exist in the IRES [16, 19]. However, we found a significant importance of IRES mutations in resistant HCV clones by selecting patients carefully and isolating the specific mutations for SVRs or non-SVRs.

Among the patients hospitalized at the Kurume University Hospital from 2001 to 2003, seven patients demonstrating HCV genotype 1b with a high viral load (>100 Kilo International Units/ml (KIU/ml) by Amplicor-HCV monitor ver. 2; Roche Molecular Diag. Co., Tokyo, Japan) were included in this study. These patients were carefully selected according to the selection standard, i.e. the patients underwent the standard treatment protocol of IFN–ribavirin therapy. There were no patients with a reduction of drug or a discontinuation of the therapy. Informed consent for this therapy was obtained from every patient, and the study was conducted in accordance with the ethical guidelines of the 1975 Declaration of Helsinki. We measured the amount of HCV RNA from patients' sera regularly during the treatment for 6 months (Fig. 1) and divided them into two groups, SVR and non-SVR. An SVR was defined as a patient in whose serum HCV RNA was not detected for at least 6 months after the end of the treatment. A non-SVR was defined as a patient in whom HCV RNA levels were reduced slightly but a high level was retained in the serum within 6 months of the end of the treatment. Three of the patients (Pt4, Pt5, and Pt6) were SVRs, while the other patients (Pt1, Pt2, Pt3, and Pt7) were non-SVRs. The HCV RNA levels in the SVRs decreased dramatically to around the lower detection limit within a week. Although the HCV RNA levels in non-SVRs decreased slowly, they remained high for at least 2 weeks.

In order to address the question of whether the IRES correlates with the clinical outcome of HCV, we compared the nucleotide sequence of the IRES between the SVRs and non-SVRs. The patients' sera were collected at pre-treatment 0 and 2 weeks after the start of therapy. Viral RNA was extracted from the serum, and IRES cDNA was obtained by nested RT-PCR. To detect all variations of the IRES, primer cocktail (5′-GCACACCCAACCTGGGGC CC-3′, 5′-CGAGGTTGCGACCGCTCGGAAG-3′, 5′-GA AGCCGCATGTGAGGGTATCGATGAC-3′) was used for reverse transcription. PCR was performed for 35 cycles (94°C, 30 s; 55°C, 30 s; 72°C, 60 s) after pre-heating (94°C, 2 min) using an outer primer pair (5′-GGGGCGA CACTCCACCATAG-3′, 5′-GATCTGACCACCGCCCGG

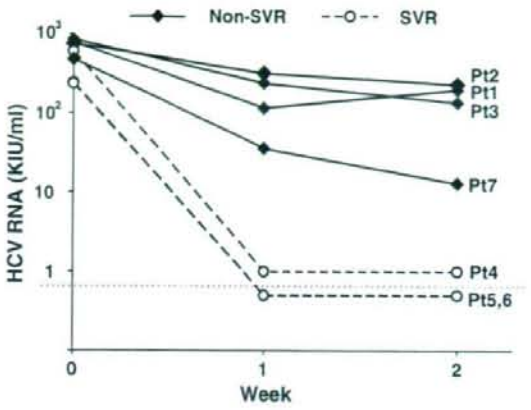

Fig. 1 Viral RNA kinetics in chronically HCV-infected patients undergoing interferon–ribavirin therapy. The *solid* and *dashed lines* indicate the kinetics of the amount of RNA from non-SVRs (*solid diamond*) and SVRs (*open circle*), respectively. The *dashed lines* from two patients' data at the bottom are overlapping. *Horizontal dotted line* shows the limit of detection by Amplicor-HCV monitor ver. 2. All patients received intramuscular IFNα-2b (Intron, Schering-Plough, Kenilworth, NJ) in combination with a daily oral 600–800 mg dose of ribavirin for 24 weeks. For the first 2 weeks of the combination therapy, 6 MU of IFNα-2b were given daily. The IFN dosing frequency was then reduced to 6 MU three times a week for the remaining 22 weeks. The ribavirin dosage was 600 mg daily for the patients who weighed less than 60 kg and 800 mg daily for patients who weighed between 60 and 80 kg

GAAC-3′), and then incubated at 72°C for 10 min. This cycle was again performed under the same conditions using an inner primer pair (5′-GTTTTTCTTTGAGGTTTAGG-3′, 5′-ACACTCCACCATAGATCACTC-3′). The final PCR product of 352 bp was cloned using TA cloning vector (pT7Blue-2, Novagen, USA), and three independent clones from each patient were sequenced (sequencer Model 310, ABI, USA).

IRES sequences of SVRs at 1 and 2 weeks after the start of therapy were unavailable because the amount of RNA was below or near the detection limit, and RNA could not be isolated, although the RNAs were detected by Amplicor-HCV monitor ver. 2, which is one of the qualitative assays with high sensitivity. The mutations specific to the non-SVRs, at pre-treatment (0W) and 2 weeks after the start of therapy (2W), are shown in Fig. 2. The distribution of mutations is summarized in Table 1, including the mutations specific to the SVRs at pre-treatment (0W). For pre-treatment (0W), the distribution of mutations was similar when SVRs and non-SVRs were compared (Table 1), with the exception that mutations were also found in dII in all clones from patient 3 (non-SVR). Previous therapy with IFN might be related to mutation in dII, since patient 3 has a history of IFN monotherapy. In comparison with pre-treatment (0W) and 2 weeks (2W)

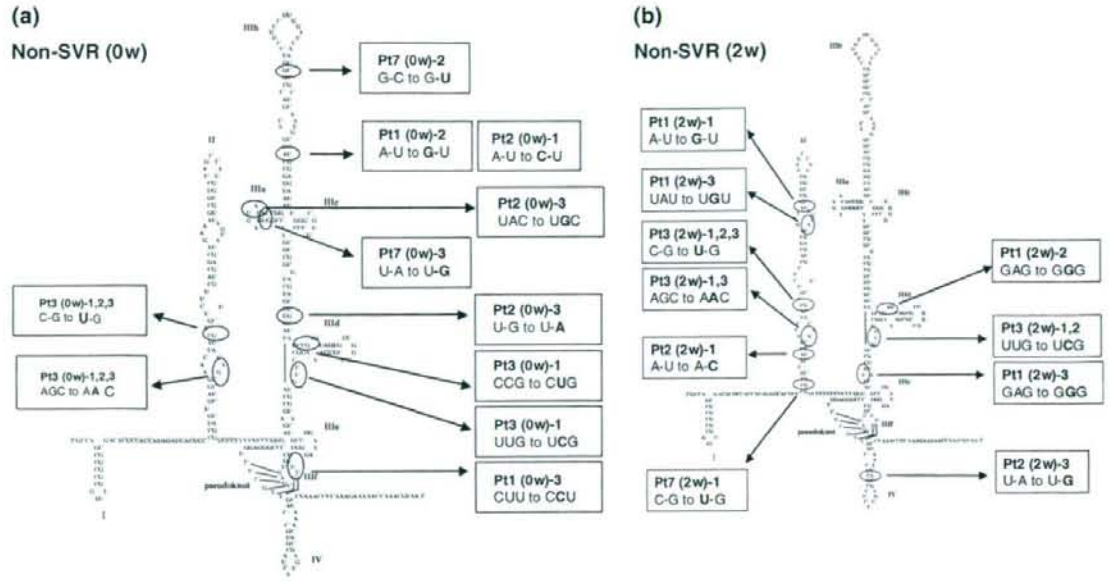

Fig. 2 The nucleotide sequence and predicted secondary structure of the HCV IRES. The nucleotide sequence shows the consensus sequence which was found among SVRs 0 weeks, non-SVRs 0 weeks and non-SVRs 2 weeks. The secondary structure is based on the HCV-JS strain [5]. The original structure is not changed for simplification of the figure, although several base pairings are partly disrupted due to the mutations. The numbers following Pt indicate the patients and each clone number from same patient. The number in brackets shows the week after the start of treatment. The position of mutations found is indicated in the *circle*. **a** Non-SVR-specific heterogeneity at pre-treatment 0 weeks. **b** Non-SVR-specific heterogeneity at 2 weeks after the start of therapy

Table 1 Number of mutations in non-SVRs and SVRs

		SVRs	Non-SVRs	
		0 weeks[a]	0 weeks	2 weeks
dII	UM[b]	0	1	4
	NM	0	1	2
	SM	0	0	0
	Total	0	2	6
dIII	UM	4	5	0
	NM	3	3	3
	SM	0	1	0
	Total	7	9	3
dIV	UM	0	0	1
	NM	1	0	0
	SM	0	0	0
	Total	1	0	1

[a] Week after the start of therapy

[b] *UM* unstable mutation, *NM* null mutation or *SM* (stable mutation) mean mutations that would disrupt the base pairing, not affect the base pairing, or form potential base pairing, respectively

after the start of therapy, in non-SVRs, the number of mutations in dII increased from 2 to 6 (Table 1, and compare Fig. 2a, b). Conversely, the number of mutations in dIII decreased from 9 to 3. These results indicate that mutation was preferentially shifted from dIII to II in non-SVRs during the therapy. It was also noted that the number of mutations which would disrupt the base pairing (referred to as UM in Table 1) in dII increased from 1 to 4, whereas those in dIII decreased from 5 to 0 (Table 1). This suggests that the mutational shift from dIII to II might disrupt several base pairings in dII but restore the base pairing in dIII. Non-SVR clones at 2 weeks after the therapy showed a decreased translational activity using a luciferase reporter gene assay (data not shown). This indicates that the mutational shift from dIII to II in non-SVRs leads to a decrease in viral translational activity.

Recently, comparing the IRES sequences of non-SVRs with those of SVRs, a few specific nucleotide substitutions have been observed [14, 16, 19]. No clinically significant variations have been reported in the IRES. However, we found a relationship between IRES mutations and clinical outcome. The discrepancy between previous reports and our results may be ascribed to several methodological differences. First, we selected the patients in order to obtain a uniform background of patients using strict criteria. Second, we extracted unique mutations specific for SVRs or non-SVRs in order to identify the principal mutations. Our study demonstrates that mutation was preferentially

shifted from dIII to II in non-SVRs during IFN–ribavirin therapy. Moreover, a similar tendency of mutational shift was observed with patients currently undergoing therapy with PegIFN–ribavirin (data not shown), suggesting a relationship between IRES mutation and clinical outcome.

It is apparent that the accumulation of unstable mutations in dIII shifts to that of unstable mutations in dII during treatment (Table 1). The same result was also obtained using a new IRES structure model [10] instead of using the previous model described in this study (Fig. 2). dIII has been reported to directly bind to the ribosome to stabilize the IRES-ribosome complex, whereas dII is involved in triplet decoding and therefore does not bind to the ribosome directly [9, 15]. It is thus possible that a mutation in dIII rather than dII may dramatically change the ribosome binding activity, e.g. the release of the IRES from the ribosome, and the degradation of free IRES and HCV RNA [11] or vice versa. Why does the dIII mutant in SVRs and non-SVRs accumulate before treatment? It may be partly because dIII mutant has a dominant trait, e.g. the translational activity of the dIII mutant is higher than that of the dII mutant (data not shown). And why are dIII mutants in SVRs and non-SVRs sensitive to therapy? dIII mutant may exist at the error threshold point, as suggested by the error catastrophe theory regarding viruses [1]. Therefore, if drugs that perturb the viral load, e.g. ribavirin and IFN, are added, then the clone may rapidly disappear with, for example, catastrophic breakdown of the ribosome-dIII complex. On the contrary, dII mutant may have recessive trait, e.g. inefficient translational activity (data not shown). However, this trait, conversely, might be an advantage for escape from the immune system, because inefficient translational activity might lead to a reduction in the number of viral proteins that are recognized by immune cells. An HCV variant containing a dIII deletion in the IRES, described in a previous report [13], might be the extreme escape mutant.

It has generally been thought that the decay curve of HCV in patients undergoing combination therapy with IFN–ribavirin basically exhibits a biphasic pattern in both SVRs and non-SVRs [3]. The decay curve of HCV in this study also seems to be biphasic: the first phase with a rapid decrease during 0–7 days, and the second phase with a slower decrease after 7 days (Fig. 1) except Pt1 (non-SVR). HCV in patients is a mixture of genetically distinct variants known as quasispecies. We speculate that HCV is composed of several variants before therapy, including mutations in dII that are resistant to therapy and in dIII that are sensitive to therapy. Particularly in non-SVRs, dIII mutant might be predominant and excluded rapidly in the first phase, whereas the dII mutants may exist as a small population in the first phase, resist the therapy, become a predominant population, and show slower decrease in the second phase. Theoretically, it is unlikely that a dII mutant would be directly derived from a dIII mutant, because such mutants would require simultaneous mutations in a short period: firstly a preferential mutation in dII, and secondly a selective mutation which reverts to the original dIII. On the other hand, in SVRs, the population size of the dIII mutant would be larger than that of the non-SVRs before therapy, and thus the decay curve shows a more rapid decrease than that of the non-SVRs. The dII mutant in SVRs may be a much smaller population than that in non-SVRs, possibly below or near the detection limit by PCR.

We propose that dII might be a potential target for antiviral therapy to improve long-lasting therapy. Indeed, siRNAs specific for highly conserved regions of HCV, including dII, inhibited virus translation and subgenomic replication in cultured cells [7]. The siRNA specific for the mutated position in dII might suppress dII mutant clones and shorten the length of therapy. Also, a determination of the IRES sequence in the dII mutant before therapy should be useful for the prediction of drug response and rapid design of siRNAs.

Acknowledgments We would like to thank to T. Sayano (Kyushu University), K. Yasuda (Department of Parasitology, Kurume University School of Medicine) and Y. Imamura (Division of Infectious Diseases, Department of Infectious Medicine, Kurume University School of Medicine) for their valuable technical assistance. We also thank T. Omura for his critical reading of the manuscript.

References

1. Eigen M (2002) Error catastrophe and antiviral strategy. Proc Natl Acad Sci USA 99:13374–13376
2. Fauquet CM, Mayo MA, Maniloff J, Desselberger U, Ball LA (2005) Virus taxonomy. Eighth Report of the International Committee on Taxonomy of Viruses, Elsevier Academic Press, London
3. Herrmann E, Zeuzem S (2006) The kinetics of hepatitis C virus. Eur J Gastroenterol Hepatol 18:339–342
4. Honda M, Ping LH, Rijnbrand RC, Amphlett E, Clarke B, Rowlands D, Lemon SM (1996) Structural requirements for initiation of translation by internal ribosome entry within genome-length hepatitis C virus RNA. Virology 222:31–42
5. Honda M, Beard MR, Ping LH, Lemon SM (1999) A phylogenetically conserved stem-loop structure at the 5′ border of the internal ribosome entry site of hepatitis C virus is required for cap-independent viral translation. J Virol 73:1165–1174
6. Kieft JS, Zhou K, Jubin R, Murray MG, Lau JY, Doudna JA (1999) The hepatitis C virus internal ribosome entry site adopts an ion-dependent tertiary fold. J Mol Biol 292:513–529
7. Korf M, Jarczak D, Beger C, Manns MP, Kruger M (2005) Inhibition of hepatitis C virus translation and subgenomic replication by siRNAs directed against highly conserved HCV sequence and cellular HCV cofactors. J Hepatol 43:225–234
8. Kumagai N, Takahashi N, Kinoshita M, Tsunematsu S, Tsuchimoto K, Saito H, Ishii H (2004) Polymorphisms of NS5B protein relates to early clearance of hepatitis C virus by interferon plus ribavirin: a pilot study. J Viral Hepat 11:225–235

9. Lukavsky PJ, Otto GA, Lancaster AM, Sarnow P, Puglisi JD (2000) Structures of two RNA domains essential for hepatitis C virus internal ribosome entry site function. Nat Struct Biol 7:1105–1110
10. Lukavsky PJ, Kim I, Otto GA, Puglisi JD (2003) Structure of HCV IRES domain II determined by NMR. Nat Struct Biol 10:1033–1038
11. Lytle JR, Wu L, Robertson HD (2001) The ribosome binding site of hepatitis C virus mRNA. J Virol 75:7629–7636
12. Martell M, Esteban JI, Quer J, Genesca J, Weiner A, Esteban R, Guardia J, Gomez J (1992) Hepatitis C virus (HCV) circulates as a population of different but closely related genomes: quasispecies nature of HCV genome distribution. J Virol 66:3225–3229
13. Revie D, Alberti MO, Braich RS, Bayles D, Prichard JG, Salahuddin SZ (2006) Discovery of significant variants containing large deletions in the 5′UTR of human hepatitis C virus (HCV). Virol J 3:82
14. Soler M, Pellerin M, Malnou CE, Dhumeaux D, Kean KM, Pawlotsky JM (2002) Quasispecies heterogeneity and constraints on the evolution of the 5′ noncoding region of hepatitis C virus (HCV): relationship with HCV resistance to interferon-alpha therapy. Virology 298:160–173
15. Spahn CM, Kieft JS, Grassucci RA, Penczek PA, Zhou K, Doudna JA, Frank J (2001) Hepatitis C virus IRES RNA-induced changes in the conformation of the 40s ribosomal subunit. Science 291:1959–1962
16. Thelu MA, Drouet E, Hilleret MN, Zarski JP (2004) Lack of clinical significance of variability in the internal ribosome entry site of hepatitis C virus. J Med Virol 72:396–405
17. Tsukiyama-Kohara K, Iizuka N, Kohara M, Nomoto A (1992) Internal ribosome entry site within hepatitis C virus RNA. J Virol 66:1476–1483
18. Wang C, Sarnow P, Siddiqui A (1993) Translation of human hepatitis C virus RNA in cultured cells is mediated by an internal ribosome-binding mechanism. J Virol 67:3338–3344
19. Yamamoto C, Enomoto N, Kurosaki M, Yu SH, Tazawa J, Izumi N, Marumo F, Sato C (1997) Nucleotide sequence variations in the internal ribosome entry site of hepatitis C virus-1b: no association with efficacy of interferon therapy or serum HCV-RNA levels. Hepatology 26:1616–1620

Tohoku J. Exp. Med., 2008, **214**, 121-128

Antimicrobial Effect of Fluoroquinolones for the Eradication of Nontypeable *Haemophilus Influenzae* Isolates within Biofilms

CHIHARU KAJI,[1] KIWAO WATANABE,[1] MICHAEL A. APICELLA[2] and HIROSHI WATANABE[3]

[1]Department of Internal Medicine, Institute of Tropical Medicine, Nagasaki University, Nagasaki, Japan
[2]Carver College of Medicine, Department of Microbiology, The University of Iowa, Iowa City, IA, USA
[3]Division of Infectious Diseases, Department of Infectious Medicine, Kurume University School of Medicine, Fukuoka, Japan

Biofilms can be defined as communities of microorganisms attached to a surface. Those bacterial biofilms cause serious problems, such as antibiotic resistance and medical device-related infections. Nontypeable *Haemophilus influenzae* (NTHi) is an important pathogen in respiratory infections, as it forms biofilms both in vitro and in vivo such as human middle ear. Recent reports indicate that otitis media, paranasal sinusitis and lower respiratory tract infections caused by *Haemophilus influenzae* have become more difficult to treat with oral antibiotic therapy. However, there has been no attention given to antibiotic eradication of NTHi biofilm. To investigate the antimicrobial effect of various antibiotics against NTHi biofilm formation, we conducted the following comparative study using both β-lactamase-negative ampicillin (AMP)-susceptible (BLNAS) and AMP-resistant (BLNAR) NTHi strains. In a microtiter biofilm assay, both levofloxacin and gatifloxacin, of the fluoroquinolone antibiotic group, significantly inhibited biofilm formation by BLNAS and BLNAR NTHi in a dose-dependent fashion compared to ampicillin of the penicillin antibiotic group, cefotaxime of the cephalosporin antibiotic group, and both erythromycin and clarithromycin of the macrolide antibiotic group. Furthermore, in flow cell chamber studies, confocal laser scanning microscopy counted survival bacteria in mature biofilm had been treated with gatifloxacin, ampicillin, cefotaxime and erythromycin. Only gatifloxacin completely killed the BLNAR NTHi isolates within biofilms without regard to the thickness of biofilm formation. The results of this study suggest that fluoroquinolones potentially have a role in therapy against diseases caused by both BLNAS and BLNAR NTHi isolates within biofilms. ——— *H. influenzae*; BLNAS; BLNAR; biofilm; fluoroquinolone; ceftriaxone; ampicillin; macrolide.

Tohoku J. Exp. Med., 2008, **214** (2), 121-128.

Received December 20, 2007; revision accepted for publication January 8, 2008.
Correspondence: Dr. Hiroshi Watanabe, Division of Infectious Diseases, Department of Infectious Medicine, Kurume University School of Medicine, 67 Asahi-machi, Kurume, Fukuoka 830-0011, Japan.
e-mail: hwata@med.kurume-u.ac.jp

Nontypeable *Haemophilus influenzae* (*H. influenzae*) is a gram-negative, pleomorphic bacterium that colonizes the human nasopharynx. NTHi can cause a variety of infections, including otitis media, sinusitis, conjunctivitis, bronchitis, and pneumonia (Murphy and Apicella 1987; Koyama et al. 2007). Recent reports state that β-lactamase-negative ampicillin (AMP)-resistant (BLNAR) strains have increased in some countries (Suzuki et al. 2003; Castanheira et al. 2006; Sunakawa and Farrell 2007), although their global prevalence remains low (Hoban and Felminghan 2002). Resistance in BLNAR strains results from mutations in the *ftsI* gene-encoding, penicillin-binding protein (*pbp*) 3, which mediates septal peptidoglycan synthesis (Hasegawa et al. 2004). Recent reports indicate that otitis media, paranasal sinusitis and lower respiratory tract infection caused by *H. influenzae* have become more difficult to treat with oral antibiotics therapy (Kaczmarek et al. 2004).

Biofilm is a structured community of bacterial cells enveloped in a self-produced, extrapolymeric matrix that is adherent to surfaces (Costerton et al. 1999; O'Toole et al. 2000). Bacterial biofilms are recognized as important causes of a variety of human infections, including infections of prosthetic devices, endocarditis, dental caries, pneumonia in cystic fibrosis, prostatitis and others (Singh et al. 2000; Donlan et al. 2001). It is well known that bacteria within biofilms are more resistant to antibiotic therapy than are planktonic organisms (Slinger et al. 2006). In order to develop strategies for the treatment of infections caused by bacteria in biofilms, including otitis media, it is important to elucidate the characteristics of bacterial pathogens within biofilms.

Recent reports state that NTHi forms biofilms both in vitro and in vivo, suggesting that biofilm formation in vivo might play an important role in the pathogenesis and chronicity of otitis media (Greiner et al. 2004; Jurcisek et al. 2005; Hall-Stoodley et al. 2006). Very little information is available concerning the effectiveness of various antimicrobials for the eradication of NTHi within biofilms. The aim of our study is to evaluate the antimicrobial effect of a variety of antibiotics on NTHi biofilms.

Materials and Methods

Bacterial strains and culture conditions

The H99 and H01 strains were clinical isolates obtained from different patients with respiratory tract infections. Before this experiment, microtiter biofilm assay was performed in each of approximately 20 BLNAS and 20 BLNAR strains obtained from different patients. The H99 and H01 strains were selected, because these strains had formed biofilms equally well. NTHi strains were reconstituted from frozen stocks and propagated on brain heart infusion (BHI) agar, or medium (Difco Laboratories, Detroit, MI, USA) supplemented with 10 μg/ml of hemin (Sigma Chemical Co., St. Louis, MO, USA) and 10 μg/ml of β-nicotinamide-adenine nucleotide (β-NAD) (Sigma) at 37°C and 5% CO_2 (Anderson et al. 1972).

Serotyping and PCR

H99 and H01 strains were serotyped by slide agglutination with antisera purchased from Difco Laboratories (Detroit, MI, USA). PCR was carried out for *H. influenzae* isolates by using mixed primers including the following (Wakunaga Pharmaceutical Co., Hiroshima): P6 primers to amplify the *p6* gene, which encodes the P6 membrane protein specific for *H. influenzae*; TEM-1 primers to amplify a part of the *β-lactamase* (*bla*) $_{TEM-1}$ gene; *pbp*3-1 primers to identify the same substitution as the low-BLNAR strains in the *fts I* gene; and *pbp* 3-2 primers to identify the same substitution as the BLNAR strains in the *fts I* gene (Hasegawa et al. 2004).

Antimicrobial susceptibility test

Minimum Inhibitory Concentrations (MICs) were determined using a broth microdilution method, according to guidelines from the Clinical and Laboratory Standards Institute (2007). Susceptibility of NTHi strains to the following 6 antibiotics was evaluated: ampicillin (AMP, Wako Pure Chemical Industries, Ltd., Osaka), cefotaxime (CTX, Wako), erythromycin (ERY, Dainippon Pharmaceutical Co., Osaka), clarithromycin (CLR, Abbott Japan Co., Tokyo), levofloxacin (LVX, Daiichi Sankyo Co., Ltd., Tokyo) and gatifloxacin (GAT, Kyorin Pharmaceutical Co., Tokyo). The antibiotics evaluated were those commonly approved for the treatment of bacterial infections from NTHi.

Microtiter biofilm assay

Biofilm formation in the H99 and H01 strains were assessed using a 96-well microplate, as previously described (Murphy and Kirkham 2002; Greiner et al. 2004). After being cultured for 48 hrs, the biofilms were exposed for 1 hr to differing concentrations (0.1 x MIC, 1 x MIC and 10 x MIC) of each antibiotics (AMP, CTX, ERY, CLR, LVX and GAT) solution every 12 hrs for 2 days (totally 4 doses). The evaluation of biofilm was performed immediately after the final exposure to the antibiotics solution. The culture medium containing planktonic cells was stained with 1% crystal violet at room temperature. After rinsing with water three times, the dye bound to the biofilm was extracted with 230 μl of 95% ethanol for 15 min. The extracted dye was quantified by measuring the absorbance at 600 nm (OD600) with a microplate reader. The strains were tested in quadruplicate for each experiment and the results were reported as three different experiments.

Biofilm growth in continuous flow cell chamber

Biofilms were formed in continuous flow cell chambers as described by Davies et al. (1998). The BLNAR H01 strain was grown in RPMI 1640 medium (Gibco BRI, Grand Island, NY, USA) supplemented with 1 μg/ml of protoporphyrin IX which is hemin without iron, 0.1 mg/ml of hypoxanthine, 0.1 mg/ml of uracil, 10 μg/ml of β-NAD, 0.8 mM of sodium pyruvate and 100 μM sialic acid, or supplemented BHI medium. The culture was diluted to an optical density (OD) of 0.15 at 600 nm and supplemented with RPMI 1640 medium. The cell suspensions of 1×10^8 colony-forming unit (cfu) /ml was used to inoculate a 37 × 5 × 5 mm flow cell chamber, filled with the prepared inoculum and incubated at 37°C for 1 hr to allow adherence to the glass coverslips (Seib et al. 2007). The chambers were then incubated for 48 hrs under 125 μl/min flow in supplemented fresh RPMI 1640 or BHI medium diluted 1:10 with sterile phosphate-buffered saline (PBS). After being cultured for 48 hrs, the biofilms were exposed for 1 hr to differing concentrations (0.1 x MIC, 1 x MIC and 10 x MIC) of each antibiotics (AMP, CTX, ERY and GAT) solution every 12 hrs for 2 days (totally 4 doses). After each exposure, the medium-containing antibiotic was replaced with fresh medium containing no antibiotic. Approximately 5 hrs after the final exposure to antibiotic solution, the biofilms were tested using a Dead/Live BacLight viability stain kit (Molecular Probes, Eugene, OR, USA), following the manufacturer's protocol, by counting the colonies.

Colony counting NTHi isolates within biofilms

To determine the antimicrobial effect of each antibiotics against NTHi isolates within biofilms, colony counting was performed after 48 hrs. To collect bacteria from the culture, the biofilms were removed from the flow chambers by flushing twice with 1 ml of sterile PBS at the end of each experiment. These washes were combined and aliquots (0.1 ml) of the suspension that had been subjected to serial 10-fold dilutions. These aliquots were sub-cultured onto supplemented BHI agars incubated at 37°C. The resultant colonies were counted to determine surviving colony-forming units ($n = 3$) at 48 hrs.

Quantification of biofilm structures

To evaluate the viability of biofilm structure after exposure to antibiotics, the biofilm formations were analysed by COMSTAT (BioCentrum-DTU, Lungby, Denmark) (Heydorn et al. 2000; Seib et al. 2007). COMSTAT is a program for quantification of three-dimensional biofilm structures. It analyzes stacks of images acquired with confocal laser scanning microscopy (CLSM). First, biofilms were stained using a Live/Dead BacLight bacterial viability stain kit (Molecular Probs, Eugene, OR, USA). This permits visualization of live and dead bacteria within the biofilms. Briefly, SYTO 9 and propidium iodide were mixed at a 1:1 ratio in sterile PBS solution. The staining solution was introduced into the chamber for 15 min at 37°C in the dark. Biofilm bacteria within the chamber were immediately visualized with CLSM (Nicon DIGITAL ECLIPSE C1, Nikon, Melville, NY, USA) using a modified stage. Three independent biofilm experiments were performed and at least four stacked images at 200 x magnification per experiment were obtained and average values were used for statistical analyses. Each of the four stacked images was selected from an apical surface area at random in the chamber and examined. The threshold value that best fit all image stacks of a trial was chosen and kept consistent for all stacks within the trial. Images were acquired at 2.0 μm intervals down through the biofilm Z-stack (μm). Therefore, the number of images in each stack varied according to the biomass and average thickness of the biofilm (Starner et al. 2006). Quantification of biofilm biomass and average thickness was calculated using a MatLab 5.3 (The MathWork, Inc., Natick, MA, USA), equipped with an Image Processing Toolbox and COMSTAT analysis. The image stacks of

"without" and "with" following exposure to each concentration of the antibiotic medium groups were averaged and compared.

Statistical tests and data analysis

All analyses of statistical significance were performed with one-tailed Student's *t*-tests using Microsoft Excel (Microsoft Corp., Redmond, WA, USA). *P* values less than were considered statistically significant. For quantification of biofilm mass, each datapoint used was the mean biomass of four randomly imaged areas from a single biofilm. Mean biomass values from different biofilm experiments were used for further statistical analyses (Starner et al. 2006).

Results

Characteristics of strains

The H99 and H01 strains used in this study are listed in Table 1. The H99 and H01 strain were both nontypeable as assayed by slide agglutination with antisera. The MIC of H99 against AMP was 0.06 mg/l and H99 did not have the mutation of *pbp* 3-1 and *pbp* 3-2 by PCR, whereas the MIC of H01 against AMP was 1.0 mg/l and H01 had the mutation of *pbp* 3-1 and *pbp* 3-2 by

TABLE 1. MICs of antibiotics and resistant gene in this study.

Strain	MIC (mg/L)						Resistant gene by PCR[g]		
	AMP[a]	CTX[b]	ERY[c]	CLR[d]	LVX[e]	GAT[f]	TEM-1	*pbp*3-1	*pbp*3-2
H-99	0.06	0.06	0.5	2.0	≦ 0.06	≦ 0.06	-	-	-
H-01	1.0	0.25	1.0	8.0	≦ 0.06	≦ 0.06	-	+	+

[a]AMP, ampicillin. [b]CTX, cefotaxime. [c]ERY, erythromycin. [d]CLR, clarithromycin. [e]LVX, levofloxacin. [f]GAT, Gatifloxacin. [g]TEM-1, type β-lactamase gene; TEM-1: -, None.
Penicillin binding protein genes; *pbp*3-1 and *pbp*3-2: +, altered; -, not altered.

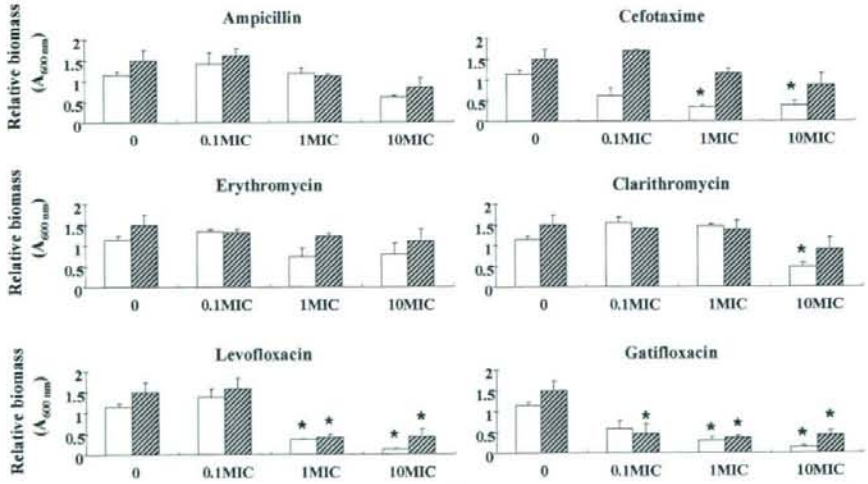

Fig. 1. Antimicrobial effect of 6 antibiotics against NTHi isolates within biofilms between BLNAS (H99, white bars) and BLNAR (H01, diagonally striped bars) strains by microtiter biofilm assay.
1 x and 10 x MIC of cefotaxime, and 10 x MIC of clarithromycin significantly inhibited only the BLNAS NTHi biofilms. By comparison, 1 x and 10 x MIC of levofloxacin and gatifloxacin inhibited both the BLNAS and BLNAR NTHi biofilms. Results are given as the average of 3 replicates with each performed in quadruplicate ± S.D.
$p < 0.001$ as compared with the same strain without exposure to antibiotics.

PCR. As a result, it was determined that H99 was a BLNAS and H01 was a BLNAR strain.

Antimicrobial effect of antibiotics against BLNAS and BLNAR NTHi biofilms by microtiter biofilm assay

The antimicrobial effect of 6 antibiotics against BLNAS and BLNAR NTHi biofilms were measured by microtiter biofilm assay (Fig. 1). As can be seen, 1 x and 10 x MIC of CTX, and 10 x MIC of CLR significantly inhibited only the BLNAS (H99) NTHi biofilm. By comparison, 1 x and 10 x MIC of LVX and GAT inhibited both the BLNAS (H99) and BLNAR (H01) NTHi biofilms (Fig. 1).

GAT completely kills BLNAR strain within biofilms

Using a flow-cell system, the antimicrobial effects of various antibiotics against the BLNAR (H01) strain within biofilms were evaluated after exposure to 0.1 x, 1 x and 10 x MIC of AMP, CTX, ERY and GAT (Fig. 2). AMP, ERY and CTX had no effect on viability at any concentration. However, the effect of GAT against the BLNAR (H01) strain within biofilms was dose-dependent and, under the concentration of 10 x MIC, killed completely. Qualitative evaluation using CLSM indicated that the total biomass of the biofilm exposed to each concentration of AMP and CTX were significantly higher than that of GAT (Fig. 3A) as assayed by COMSTAT software. Biofilms treated with GAT had a significantly lower ($p = 0.001$) total biomass than those treated with AMP and CTX. The total biomass of the biofilm after exposure to 0.1 x and 1,0 x MICs of ERY tended to be lower than that of GAT — but not significantly lower —, however, the total biomass of the 10 x MIC ERY treated biofilm was significantly higher ($p = 0.001$) than that of GAT. The average thickness of all the biofilms was similar whether or not the organisms were treated with antibiotics (Fig. 3B).

Discussion

NTHi is one of the most prevalent pathogens associated with respiratory tract infections and thus acquisition of antimicrobial resistance raises concern. The prevalence of BLNAR strains was reported to be 2.4% in the USA between 2002 and 2003 (Heilmann et al. 2005) and 9.3% in Spain between 1998 and 1999 (Marco et al. 2001). Their global prevalence of BLNAR strains remains relatively low. However, the prevalence of BLNAR in Japan has increased rapidly, from 5.8% in 2000 to 34.5% in 2004, even in *H. influ-*

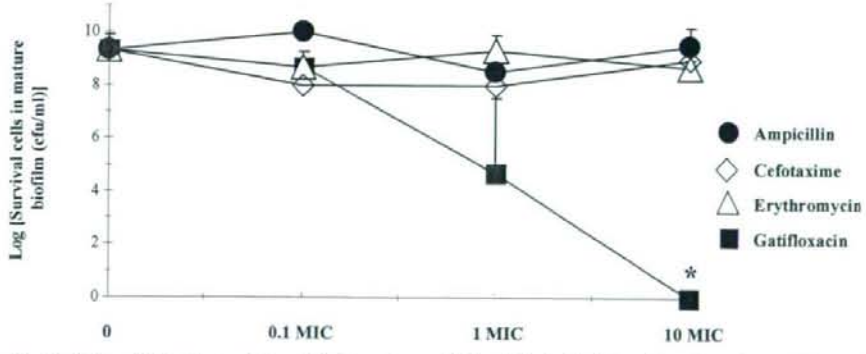

Fig. 2. Antimicrobial effect of 4 antibiotics of ampicillin (filled circle), cefotaxime (open diamonds), erythromycin (open triangles), or gatifloxacin (filled squares) against BLNAR NTHi isolate (H01) within biofilms in a continuous-flow cell chamber.
Ampicillin, erythromycin and cefotaxime had no effect on viability at any concentration, whereas the effect of gatifloxacin against the BLNAR strain within biofilms was dose-dependent and, under the concentration of 10 x MIC, killed completely. Results are given as average of 3 replicates ± S.D.
*$p < 0.001$ as compared with the strain without exposure to antibiotics.

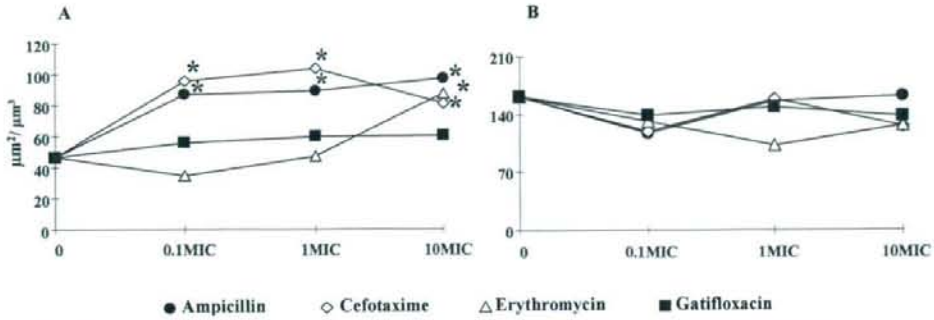

Fig. 3. Comparison of the biomass (A) and average thickness (B) of biofilms after exposure to 4 antibiotics of ampicillin (filled circle), cefotaxime (open diamonds), erythromycin (open triangles), or gatifloxacin (filled squares).
Biofilms exposed to gatifloxacin had a significantly lower total biomass than those to ampicillin and cefotaxime. The total biomass of the biofilms after exposure to 0.1 x and 1.0 x MICs of erythromycin tended to be lower than that of gatifloxacin, but the total biomass of the 10 x MIC erythromycin treated biofilm was significantly higher than that of gatifloxacin. The average thickness of all of the biofilms was similar whether or not the organisms were treated with antibiotics.
*$p < 0.001$ as compared with the strain exposed to without antibiotics.

enzae type b isolated from patients with meningitis (Hasegawa et al. 2004). The result has been an increasing number of cases of otitis media, which are difficult to treat, and an increasing incidence of treatment failures with oral antibiotics in young children (Starner et al. 2006). This is due in large part to antibiotic resistance, which points to a need for oral therapy to change along with surgical management of tympanostomy or tympanostomy tubes (Casey et al. 2004).

However, the pathogenesis of NTHi infection of airway cells involves both an intracellular life cycle as well as biofilm formation on the surface of the airway epithelia. Therefore, because NTHi invade human bronchial epithelial cells by macropinocytosis (Ketterer et al. 1999) and form biofilms both in vitro and in vivo (Greiner et al. 2004; Jurcisek et al. 2005; Hall-Stoodley et al. 2006), it is not clear whether drug resistance alone causes treatment difficulty and failure in otitis media among young children. To our knowledge, the antimicrobial effect of antibiotics against NTHi within biofilms remains unclear. Our data show that LVX and GAT have significant inhibitory effect against both BLNAS and BLNAR NTHi within biofilms compared to AMP, CTX, ERY and CLR. Our results agree with previous investigations that studied *P. aeruginosa* biofilm, as it has been shown that fluoroquinolones can penetrate exopolysaccharides (Kumon et al. 1994; Yassien et al. 1995). Since the use of fluoroquinolones in young children is limited in many countries because of adverse neurological side effects, the clinical antimicrobial effectiveness against BLNAS and BLNAR NTHi in biofilms has not been confirmed. AMP, CTX, ERY and CLR had no significant effect against either BLNAS or BLNAR NTHi biofilms, although it has been reported that macrolides have an inhibitory effect on *P. aeruginosa* biofilm formation and survival cells in biofilm (Favre-Bonté et al. 2003; Nalca et al. 2006).

There may be several limitations in the present study. First, only single BLNAS and BLNAR strains were investigated, although the biofilm formation among each of 20 BLNAS and 20 BLNAR strains were investigated before these studies and these two strains were selected. The second limitation is a lack of in vivo data.

In conclusion, our data demonstrate that fluoroquinolones could be effective therapeutic agents against biofilm diseases caused by both BLNAS and BLNAR NTHi. Further investigations, such as the chinchilla otitis media model or

clinical trial to determine the in vivo antimicrobial effect of fluoroquinolones on NTHi biofilms should be considered.

Acknowledgments

We thank M.L. Falsetta and all the staff of the Department of Microbiology, University Iowa for their help in completion of this study.

This study was funded by Health and Labour Sciences Research Grants for Research on Measures for Intractable Diseases (17243601) from the Japanese Government.

References

Anderson, P., Peter G., Johnston, R.B., Jr., Wetterlow, L.H. & Smith, D.H. (1972) Immunization of humans with polyribophosphate, the capsular antigen of *Haemophilus influenzae*, type b. *J. Clin. Invest.*, **51**, 39-44.

Casey, J.R. & Pichichero, M.E. (2004) Changes in frequency and pathogens causing acute otitis media in 1995-2003. *Pediatr. Infect. Dis. J.*, **23**, 824-828.

Castanheira, M., Gales, A.C., Pignatari, A.C., Jones, R.N. & Sader, H.S. (2006) Changing antimicrobial susceptibility patterns among *Streptococcus pneumoniae* and *Haemophilus influenzae* from Brazil: Report from the SENTRY Antimicrobial Surveillance Program (1998-2004). *Microb. Drug Resist.*, **2**, 91-98.

Clinical and Laboratory Standards Institute (2007) Performance standards for antimicrobial susceptibility testing: M100-S17, 17th informational supplement. *CLSI*, Wayne, PA.

Costerton, J.W., Stewart, P.S. & Greenberg, E.P. (1999) Bacterial biofilms: a common cause of persistent infections. *Science*, **284**, 1318-1322.

Davies, D.G., Parsek, M.R., Pearson, J.P., Iglewski, B.H., Costerton, J.W. & Greenberg, E.P. (1998) The involvement of cell-to-cell signals in the development of a bacterial biofilm. *Science*, **280**, 295-298.

Donlan, R.M. (2001) Biofilm formation: a clinically relevant microbiological process. *Clin. Infect. Dis.*, **33**, 1387-1392.

Favre-Bonté, S., Köhler, T. & Van Delden, C. (2003) Biofilm formation by *Pseudomonas aeruginosa*: role of the C4-HSL cell-to-cell signal and inhibition by azithromycin. *J. Antimicrob. Chemother.*, **52**, 598-604.

Greiner, L.L., Watanabe, H., Phillips, N.J., Shao, J., Morgan, A., Zaleski, A., Gibson, B.W. & Apicella, M.A. (2004) Nontypeable *Haemophilus influenzae* strain 2019 produces a biofilm containing N-acetylneuraminic acid that may mimic sialylated O-linked glycans. *Infect. Immun.*, **72**, 4249-4260.

Hall-Stoodley, L., Hu, F.Z., Gieseke, A., Nistico, L., Nguyen, D., Hayes, J., Forbes, M., Greenberg, D.P., Dice, B., Burrows, A., Wackym, P.A., Stoodley, P., Post, J.C., Ehrlich, G.D. & Kerschner, J.E. (2006) Direct detection of bacterial biofilms on the middle-ear mucosa of children with chronic otitis media. *JAMA*, **296**, 202-211.

Hasegawa, K., Chiba, N., Kobayashi, R., Murayama, S.Y., Iwata, S., Sunakawa, K. & Ubukata, K. (2004) Rapidly increasing prevalence of beta-lactamase-nonproducing, ampicillin-resistant *Haemophilus influenzae* type b in patients with meningitis. *Antimicrob. Agents Chemother.*, **48**, 1509-1514.

Hasegawa, K., Kobayashi, R., Takada, E., Ono, A., Chiba, N., Morozumi, M., Iwata, S., Sunakawa, K. & Ubukata, K.: Nationwide Surveillance for Bacterial Meningitis (2006) High prevalence of type b beta-lactamase-non-producing ampicillin-resistant *Haemophilus influenzae* in meningitis: the situation in Japan where Hib vaccine has not been introduced. *J. Antimicrob. Chemother.*, **57**, 1077-1082.

Heilmann, K.P., Rice, C.L., Miller, A.L., Miller, N.J., Beekmann, S.E., Pfaller, M.A., Richter, S.S. & Doern, G.V. (2005) Decreasing prevalence of beta-lactamase production among respiratory tract isolates of *Haemophilus influenzae* in the United States. *Antimicrob. Agents Chemother.*, **49**, 2561-2564.

Heydorn, A., Nielsen, A.T., Hentzer, M., Sternberg, C., Givskov, M., Ersbøll, B.K. & Molin, S. (2000) Quantification of biofilm structures by the novel computer program COMSTAT. *Microbiology*, **146**, 2395-2407.

Hoban, D. & Felmingham, D. (2002) The PROTEKT surveillance study: antimicrobial susceptibility of *Haemophilus influenzae* and *Moraxella catarrhalis* from community-acquired respiratory tract infections. *J. Antimicrob. Chemother.*, **50**, 49-59.

Jurcisek, J., Greiner, L., Watanabe, H., Zaleski, A., Apicella, M.A. & Bakaletz, L.O. (2005) Role of sialic acid and complex carbohydrate biosynthesis in biofilm formation by nontypeable *Haemophilus influenzae* in the chinchilla middle ear. *Infect. Immun.*, **73**, 3210-3218.

Kaczmarek, F.S., Gootz, T.D., Dib-Hajj, F., Shang, W., Hallowell, S. & Cronan, M. (2004) Genetic and molecular characterization of beta-lactamase-negative ampicillin-resistant *Haemophilus influenzae* with unusually high resistance to ampicillin. *Antimicrob. Agents Chemother.*, **48**, 1630-1639.

Ketterer, M.R., Shao, J.Q., Hornick, D.B., Buscher, B., Bandi, V.K. & Apicella, M.A. (1999) Infection of primary human bronchial epithelial cells by *Haemophilus influenzae*: macropinocytosis as a mechanism of airway epithelial cell entry. *Infect. Immun.*, **67**, 4161-4170.

Koyama, J., Ahmed, K., Zhao, J., Saito, M., Onizuka, S., Oma, K., Watanabe, K., Watanabe, H. & Oishi, K. (2007) Strain-specific pulmonary defense achieved after repeated airway immunizations with non-typeable *Haemophilus influenzae* in a mouse model. *Tohoku J. Exp. Med.*, **211**, 63-74.

Kumon, H., Tomochika, K., Matunaga, T., Ogawa, M. & Ohmori, H. (1994) A sandwich cup method for the penetration assay of antimicrobial agents through Pseudomonas exopolysaccharides. *Microbiol. Immunol.*, **38**, 615-619.

Marco, F., Garcia-de-Lomas, J., Garcia-Rey, C., Bouza, E., Aguilar, L., Fernandez-Mazarrasa, C. & The Spanish Surveillance Group for Respiratory Pathogens (2001) Antimicrobial susceptibilities of 1,730 *Haemophilus influenzae* respiratory tract isolates in Spain in 1998-1999. *Antimicrob. Agents Chemother.*, **45**, 3226-3228.

Murphy, T.F. & Apicella, M.A. (1987) Nontypeable *Haemophilus influenzae*: a review of clinical aspects, surface antigens, and the human immune response to infection. *Rev. Infect. Dis.*, **9**, 1-15.

Murphy, T.F. & Kirkham, C. (2002) Biofilm formation by nontypeable *Haemophilus influenzae*: strain variability, outer membrane antigen expression and role of pili. *BMC Microbiol.*, **2**, 7.

Nalca, Y., Jäsch, L., Bredenbruch, F., Geffers, R., Buer, J. & Hässler, S. (2006) Quorum-sensing antagonistic activities of azithromycin in *Pseudomonas aeruginosa* PAO1: a global approach. *Antimicrob. Agents Chemother.*, **50**,

1680-1688.
O'Toole, G., Kaplan, H.B. & Kolter, R. (2000) Biofilm formation as microbial development. *Annu. Rev. Microbiol.*, **54**, 49-79.
Seib, K.L., Wu, H.J., Srikhanta, Y.N., Edwards, J.L., Falsetta, M.L., Hamilton, A.J., Maguire, T.L., Grimmond, S.M., Apicella, M.A., McEwan, A.G. & Jennings, M.P. (2007) Characterization of the OxyR regulon of *Neisseria gonorrhoeae*. *Mol. Microbiol.*, **63**, 54-68.
Singh, P.K., Schaefer, A.L., Parsek, M.R., Moninger, T.O., Welsh, M.J. & Greenberg, E.P. (2000) Quorum-sensing signals indicate that cystic fibrosis lungs are infected with bacterial biofilms. *Nature*, **407**, 762-764.
Slinger, R., Chan, F., Ferris, W., Yeung, S.W., St. Denis, M., Gaboury, I. & Aaron, S.D. (2006) Multiple combination antibiotic susceptibility testing of nontypeable *Haemophilus influenzae* biofilms. *Diagn. Microbiol. Infect. Dis.*, **56**, 247-253.
Starner, T.D., Zhang, N., Kim, G., Apicella, M.A. & McCray, P.B., Jr. (2006) *Haemophilus influenzae* forms biofilms on airway epithelia: implications in cystic fibrosis. *Am. J. Respir. Crit. Care. Med.*, **174**, 213-220.
Sunakawa, K. & Farrell, D.J. (2007) Mechanisms, molecular and sero-epidemiology of antimicrobial resistance in bacterial respiratory pathogens isolated from Japanese children. *Ann. Clin. Microbiol. Antimicrob.*, **13**, 6-7.
Suzuki, K., Nishimura, T. & Baba, S. (2003) Current status of bacterial resistance in the otolaryngology field: results from the Second Nationwide Survey in Japan. *J. Infect. Chemother.*, **9**, 46-52.
Yassien, M., Khardori, N., Ahmedy, A. & Toama, M. (1995) Modulation of biofilms of *Pseudomonas aeruginosa* by quinolones. *Antimicrob. Agents Chemother.*, **39**, 2262-2268.

Journal of Hospital Infection (2008) 68, 262–268

Available online at www.sciencedirect.com

ScienceDirect

www.elsevierhealth.com/journals/jhin

Nosocomial outbreak of epidemic keratoconjunctivitis accompanying environmental contamination with adenoviruses

N. Hamada [a,*], K. Gotoh [a], K. Hara [a], J. Iwahashi [a], Y. Imamura [a], S. Nakamura [b], C. Taguchi [b], M. Sugita [b], R. Yamakawa [b], Y. Etoh [c], N. Sera [c], T. Ishibashi [c], K. Chijiwa [c], H. Watanabe [a]

[a] *Division of Infectious Diseases, Department of Infectious Medicine, Kurume University School of Medicine, Kurume, Japan*
[b] *Department of Ophthalmology, Kurume University Hospital, Kurume, Japan*
[c] *Fukuoka Institute of Health and Environmental Sciences, Fukuoka, Japan*

Received 7 August 2007; accepted 20 December 2007
Available online 4 March 2008

KEYWORDS
Nosocomial outbreak;
Keratoconjunctivitis;
Adenovirus; Eye drops

Summary An outbreak of acute keratoconjunctivitis involving 27 patients occurred in the Department of Ophthalmology, Kurume University Hospital. Adenoviral DNA was detected in four inpatients, one outpatient and one healthcare worker. Sequence-based typing of adenoviral DNA indicated serotype 3 from one inpatient, the rest being serotype 37. At a later stage of the outbreak adenoviral DNA types 37 and/or 3 were also detected from almost all environmental instruments and commonly used eye drops, despite thorough disinfection of the environment and enforcement of various infection control measures. The detection rate of adenoviral DNA in environmental swabs was 81%. A further second disinfection of the environment reduced the detection rate of adenoviral DNA to 38%. The outbreak ceased after closing the ophthalmology ward and outpatient consulting room, accompanied by enhanced cleaning of environmental instruments and the introduction of disposable eye drops for individual patients.

* Corresponding author. Address: Division of Infectious Diseases, Department of Infectious Medicine, Kurume University School of Medicine, Kurume 830-0011, Japan. Tel.: +81 942 31 7549; fax: +81 942 31 7697.
E-mail address: nhamada@med.kurume-u.ac.jp

0195-6701/$ - see front matter © 2008 The Hospital Infection Society. Published by Elsevier Ltd. All rights reserved.
doi:10.1016/j.jhin.2007.12.012

Introduction

Epidemic keratoconjunctivitis (EKC) due to adenoviruses is a common healthcare-associated infection, especially in ophthalmology departments. This is partly because adenovirus is highly infectious and relatively stable in the environment, but also because there are additional common risk factors for transmission in ophthalmological clinical practice. These include diagnostic instruments that may directly touch an affected eye, incomplete disinfection of instruments and the usual risk from contaminated hands of medical staff.

A healthcare-associated outbreak of EKC occurred in Kurume University Hospital in 2007. We describe the time-course of the incident and characteristics of the pathogens involved.

Methods

From February to March 2007, an outbreak of EKC occurred at the Department of Ophthalmology of Kurume University Hospital, involving 18 inpatients, seven outpatients (including three patients from another ward) and two healthcare workers. EKC infection was diagnosed clinically and/or by a rapid diagnosis (immunochromatographic) kit for detection of adenoviral antigen (Adeno Check, Santen Pharmaceutical Co. Ltd).

Adenoviral DNA was extracted from swabs of environmental instruments (Table II) and patients' conjunctiva using QIAmp DNA Mini kit (QIAGEN, Hilden, Germany) according to the manufacturer's instructions. For polymerase chain reaction (PCR), the partial hexon genes were amplified as described in previous reports.[1–5] The primer pairs are listed in Table I. PCR reactions were performed using three protocols. In the first, the amplification reaction was carried out with (i) 25 cycles of denaturation at 96 °C for 20 s, annealing at 55 °C for 20 s, and primer extension at 72 °C for 1 min, followed by (ii) 35 cycles of denaturation at 96 °C for 20 s, annealing at 55 °C for 20 s, and primer extension at 72 °C for 30 s and (iii) a final product extension at 72 °C for 10 min. In the second, a first PCR reaction was carried out with 40 cycles of denaturation at 98 °C for 10 s, annealing and primer extension at 65 °C for 6 min, followed by second PCR (40 cycles of denaturation at 94 °C for 1 min, annealing at 60 °C for 1 min, and primer extension at 72 °C for 2 min). In the third protocol, first PCR reaction was carried out with 36 cycles of denaturation at 94 °C for 1 min, annealing at 50 °C for 1 min and primer extension at 72 °C for 2 min, followed by second PCR using the same conditions as the first. PCR was performed two or three times for confirmation by using each protocol. Protocol 1 was performed in the Department of Infectious Medicine, and protocols 2 and 3 in the Fukuoka Institute of Health and Environmental Sciences. The PCR products were directly sequenced using dye terminator (BigDye, ABI, USA). The primers for the amplification were also used for sequencing reaction except in protocol 2 (Table I).

Results

Figure 1 shows the clinical history of patients in the outbreak. Most patients were identified during the late stage of the outbreak (6–15 March), with most probably infected with adenovirus during the early stages of the outbreak (20–27 February).

Table I Primers for polymerase chain reaction (PCR) of adenoviruses

Protocol		Primer	Sequence	Reference
1		Ad1A to F	TTCCCCATGGCCAYAACAC	Xu *et al.*[1]
		Ad2A to F	CCCTGGTAKCCRATRTTGTA	
2	1st PCR	Hx5–1	AAGATGGCCACCCCCTCGATGATGCCGCAGT	Takeuchi *et al.*[3]
		HX3–1	CACTTATGTGGTGGCGTTGCCGGCCGAGAACGG	
	2nd PCR	HX5–3	CACATCGCCGGACAGGATGCTTCGGAGTA	
		HX3–4	GTGTTGTGAGCCATGGGGAAGAAGGTGGC	
	Sequence	S29	GCCAGCACRTWCTTTGACAT	
	Sequence	S52	CCCATGTTGCCAGTGCTGTTGTARTACA	
	Sequence	S51	CCCAACAGACCCAAYTACAT	
	Sequence	S53	AAGGGGTTGACGTTGTCCAT	
3	1st PCR	AdTU7	GCCACCTTCTTCCCCATGGC	Saitoh-Inagawa *et al.*[4]
		AdTU4′	GTAGCGTTGCCGGCCGAGAA	
	2nd PCR	AdU–S′	TTCCCCATGGCNCAACAC	
		AdU–A	GCCTCGATGACGCCGCGGTG	

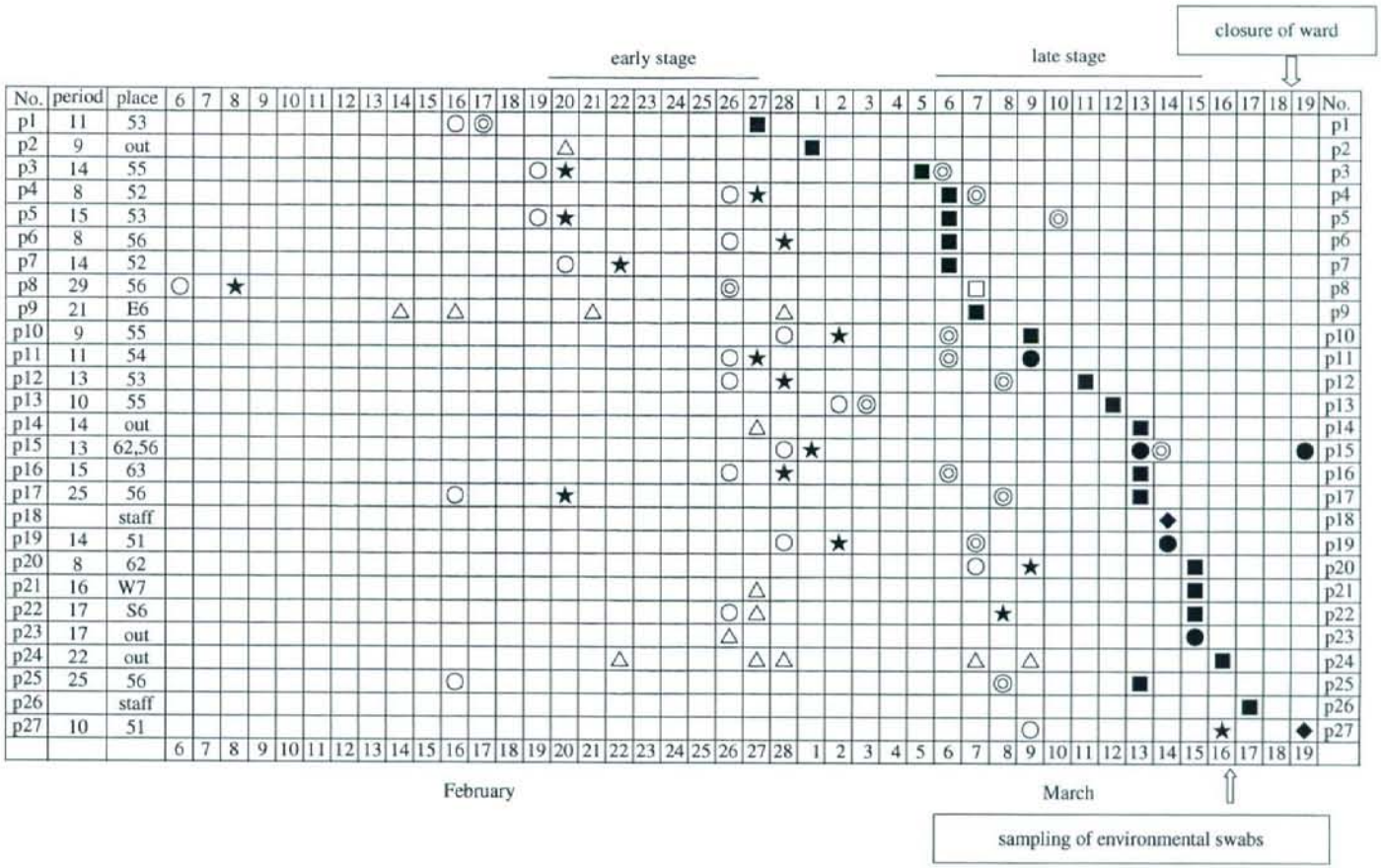

No.	period	place	6	7	8	9	10	11	12	13	14	15	16	17	18	19	20	21	22	23	24	25	26	27	28	1	2	3	4	5	6	7	8	9	10	11	12	13	14	15	16	17	18	19	No.
p1	11	53											○	◎										■																				p1
p2	9	out															△								■																				p2
p3	14	55															○	★												■	◎																p3
p4	8	52																					○	★							■	◎														p4
p5	15	53															○	★													■			◎												p5
p6	8	56																					○		★						■															p6
p7	14	52															○		★												■															p7
p8	29	56	○		★																		◎									□														p8
p9	21	E6									△		△					△							△						■															p9
p10	9	55																							○		★				◎			■											p10
p11	11	54																					○	★							◎			●											p11
p12	13	53																					○		★								◎			■									p12
p13	10	55																									○	◎								■									p13
p14	14	out																						△													■								p14
p15	13	62,56																							○	★											●	◎					●		p15
p16	15	63																					○		★						◎						■								p16
p17	25	56											○				★																◎					■								p17
p18		staff																																			◆								p18
p19	14	51																							○		★					◎						●							p19
p20	8	62																														○		★					■						p20
p21	16	W7																						△															■						p21
p22	17	S6																					○	△									★						■						p22
p23	17	out																					△																■						p23
p24	22	out																	△					△	△							△		△						■						p24
p25	25	56											○																				◎						■							p25
p26		staff																																								■				p26
p27	10	51																																○							★			◆		p27
			6	7	8	9	10	11	12	13	14	15	16	17	18	19	20	21	22	23	24	25	26	27	28	1	2	3	4	5	6	7	8	9	10	11	12	13	14	15	16	17	18	19	

Figure 1 Temporal relationship between contact and onset of symptoms during outbreak. Period: days between contact and onset; Place: room number of inpatient ('out' means outpatient; 'alphabet + number' means inpatient of other ward.). Blank in period column indicates no data. ○, admission; ◎, discharged from hospital; ★, operation; △, visit of outpatient; □, adenovirus rapid test (−); ■, adenovirus rapid test (+); ◆, adenoviral DNA (+); ●, adenovirus rapid test (+) and adenoviral DNA (+).

Figure 2 shows the electrophoretic pattern of PCR products from various environmental swabs during the later stages of the outbreak. The number in Figure 2 corresponds to samples tested (Table II). Adenoviral DNA was detected by protocol 1 in most samples; 17 samples out of 21 were positive (81%), despite a thorough disinfection of the environment performed just after the beginning of the outbreak. Adenoviral DNA was also detected in eye drops. A further environmental clean, performed just after closure of the ward, achieved a greater reduction of adenoviral DNA-positive instruments; eight out of 21 samples were still positive (38%). Adenoviral DNA was not detected from three control swabs taken from a neighbouring dermatology ward.

Sequence analysis showed that all amplified DNA from five patients except patient 11 (Figure 1, Table II) was identified as adenovirus type 37, similar to prototype 37 bar one mutation (Figure 3A). Identical nucleotide sequences of type 37 were also found from swabs from a slit lamp for EKC (e21), a probe from ophthalmological cryo equipment (e8), glasses frame (e6), and eye drops (e3) (Table II). Almost all the amplified adenoviral DNA from elsewhere in the environment was type 3 (Figure 3B, Table II); this was also the type recovered from patient 11. In addition, type 3 as well as type 37 adenovirus was identified from a glasses frame (e6) and types 2 and 3 were recovered from swabs from a treatment room tap (e19) (Table II).

Discussion

Adenoviral conjunctivitis is mainly caused by adenovirus types 3, 4, 8, 19 and 37, with types 8, 19 and 37 associated with comparatively severe conjunctivitis.[6] In a previous report, the genome of adenovirus type 37 was suggested to be comparatively evolutionarily stable.[7] The type 37 described in our report was closely related to the adenovirus type 37 prototype (Figure 3A). However, recent long-term surveillance has shown a genetic variation of type 37, suggesting annual transition of type 37 variants.[8,9]

The region sequenced in this study for comparison was a part of hypervariable regions (HVRs) of the hexon gene, which shows genetic variation among strains. The nucleotide sequences of adenovirus type 37, which were confirmed in swabs from both environment and patients, were identical without mutations, although the whole sequence was not examined. We concluded that the outbreak was principally caused by the same strain of adenovirus type 37.

Even after termination of the outbreak following various control measures including ward closure, most practical control measures have still not been

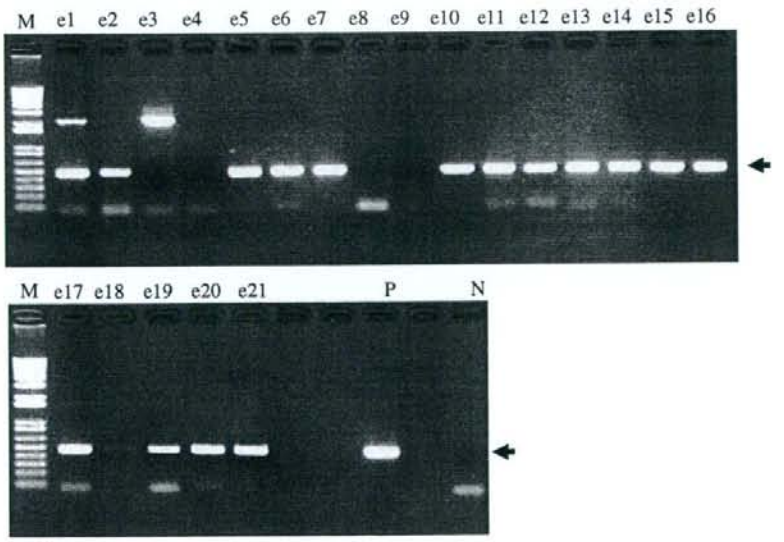

Figure 2 Polymerase chain reaction (PCR) products of various environmental swabs. P, positive control DNA; N, negative control; M, DNA size marker; arrow, expected size (482 bps) of adenoviral DNA using PCR protocol 1; alphabet + numerical number, sample number, explained in Table II.

Table II Summary of examinations of samples

Swabs from environment		PCR protocol[a]		Ad type[b]
Number	Instruments and eye drops	1	2 or 3	
e1	Applanation tonometer chip in room 1	*		3
e2	Eye drop 1 in room 1	*		3
e3	Eye drop 2 in room 1	*		37[c]
e4	Eye drop 3 in room 1			–
e5	Eye drop 4 in room 1	*		3
e6	Glasses frame for visual acuity test	*	*	3, 37
e7	Lens for visual acuity test	*		3
e8	Ophthalmological cryo equipment (probe)		*	37
e9	Ophthalmological cryo equipment			–
e10	Slit lamp of laser photocoagulation	*		3
e11	Electroretinogram (ERG) electrode	*		3
e12	Multifocal elecroretinogram (VERIS) electrode	*		3
e13	Chip of A-mode ultrasonography	*		3
e14	Pachymeter chip	*		3
e15	Pachymeter pen	*		3
e16	Room 6	*		3
e17	Fluorescein angiography (FAG) instrument in room 6	*		3
e18	Eye drop 4 in room 6	*		3
e19	Tap in treatment room	*	*	3, 2
e20	Slit lamp in room 2	*		3
e21	Slit lamp for EKC patients	*	*	37
Swabs from patient				
Number	Adenovirus rapid test			
p11	+	*		3
p15	+	*	*	37
p18	–	*	*	37
p19	+		*	37
p23	+		*	37
p27	–	*	*	37

EKC, epidemic keratoconjunctivitis.
[a] Asterisk indicates positive result by each polymerase chain reaction (PCR) protocol.
[b] Adenovirus serotype.
[c] Result obtained using protocol 2 primer pairs.

established. EKC caused by adenovirus is highly contagious and infection may rapidly spread in hospital. Ophthalmologists and nurses play an important role in outbreak prevention.

We detected adenoviral DNA in 81% of samples from the ophthalmology environment, even after disinfection (using alcohol and glutaraldehyde). After a second disinfection of the environment, the detection rate of adenoviral DNA dropped to 38%. This implies that once contamination occurs, it is difficult to eliminate adenoviral DNA from the environment. It also suggests that the outbreak was associated with wide environmental contamination by adenoviruses. This could have been the main source for person-to-person transmission. It is known that about 80% of adenovirus is naturally inactivated within a week under dry conditions.[10] Thus, even if adenoviral contamination of instruments occurred, most of the virus would have been eliminated within a week, with just slight infectivity remaining. Person-to-person transmission would have been more easily controlled by hand washing and/or wearing disposable gloves.

Adenovirus types 37 and 3 were detected in eye drops as well as from patients' swabs and environmental instruments (Table II). These eye drops were routinely exchanged every morning and shared amongst patients during the early stages of the outbreak. The minimum amount of clinically infectious adenovirus is reported to be 100 pfu.[10] Patients' swabs contained 10^{10} copies/ml, confirmed by real-time PCR. Therefore a small drop, such as tear fluid from a patient, would have contained enough viral particles to cause infection. Although we did not examine the infectivity of the contaminated eye drops, the detection of viral DNA implies a risk of direct virus transmission. Viruses are known to survive in solutions such as eye drops.[11]

Ophthalmology staff do not consider keratoconjunctivitis to be a life-threatening disease. However, lethal reactivation of latent adenovirus kidney infection in a renal transplant patient has been reported and Adenovirus type 37 has been detected in spinal fluid from a patient with encephalitis.[12] One postoperative patient (p27), who did not show any EKC symptoms, was shown to be infected with adenovirus type 37 (Figure 1). All patients, regardless of symptoms, should be treated with standard precautions.

The most critical control measures to prevent such an outbreak as described here, should be the avoidance of direct transmission of adenovirus to patients through eye drops, contaminated equipment and hands of ophthalmologists. Thorough disinfection of equipment and hands of ophthalmologists should be performed before consultation, as well as the introduction of disposable eye drops.

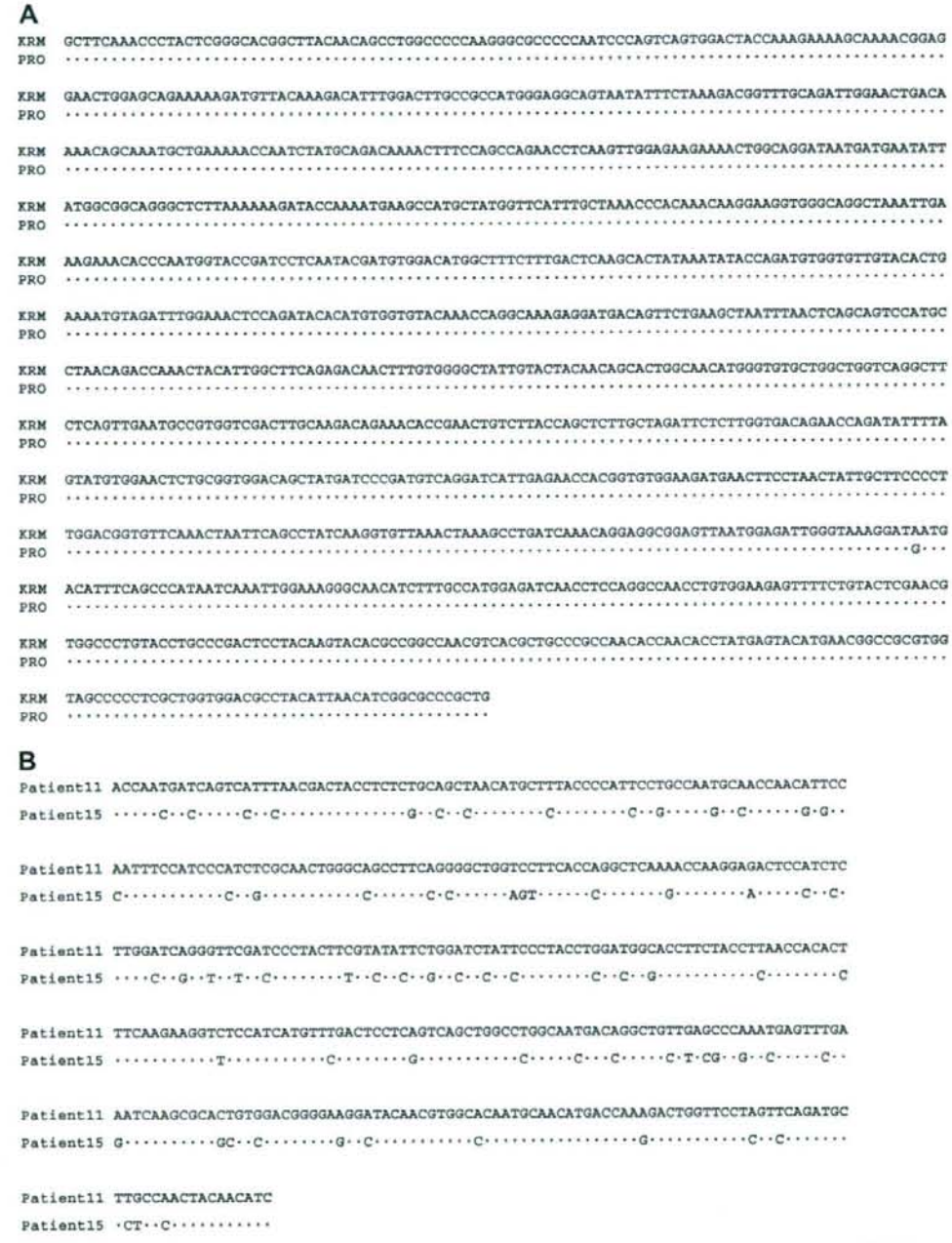

Figure 3 Comparison of sequences of amplified adenoviral DNA. (A) Alignment of adenovirus type 37 DNA between swabs from both environment and patient (KRM), and prototype strain (PRO, accession number: DQ149632). (B) Alignment of adenovirus type DNA between patient p11 (type 3) and patient p15 (type 37) described in Figure 1 and Table II.

Acknowledgements

We thank Miho Miura (ICN), Division of Infection Control and Prevention, Kurume University Hospital, for the environmental sampling.

Conflict of interest statement
None declared.

Funding sources
None.

References

1. Xu W, McDonough MC, Erdman DD. Species-specific identification of human adenoviruses by a multiplex PCR assay. *J Clin Microbiol* 2000;**38**:4114–4120.
2. He JW, Jiang S. Quantification of enterococci and human adenoviruses in environmental samples by real-time PCR. *Appl Environ Microbiol* 2005;**71**:2250–2255.
3. Takeuchi S, Itoh N, Uchio E, *et al.* Adenovirus strains of subgenus D associated with nosocomial infection as new etiological agents of epidemic keratoconjunctivitis in Japan. *J Clin Microbiol* 1999;**37**:3392–3394.
4. Saitoh-Inagawa W, Oshima A, Aoki K, *et al.* Rapid diagnosis of adenoviral conjunctivitis by PCR and restriction fragment length polymorphism analysis. *J Clin Microbiol* 1996;**34**: 2113–2116.
5. Takeuchi S, Itoh N, Uchio E, Aoki K, Ohno S. Serotyping of adenoviruses on conjunctival scrapings by PCR and sequence analysis. *J Clin Microbiol* 1999;**37**:1839–1845.
6. Sawada H, Aoki K, Kawana R, *et al.* Molecular epidemiology of adenoviral conjunctivitis in Sapporo, Japan, and Manila, the Philippines. *Jpn J Ophthalmol* 1987;**31**:538–546.
7. de Jong TA, Wermenbol AG, van der Avoort HG, Wigand R. Genome type analysis of adenovirus 37 isolates. *J Med Virol* 1988;**25**:77–83.
8. Kaneko H, Kondo T, Fujiwara T, *et al.* Clinical and virological studies of nosocomial conjunctivitis infection caused by adenovirus type 37 variant. *Nippon Ganka Gakkai Zasshi* 2005;**109**:489–496.
9. Ariga T, Shimada Y, Shiratori K, *et al.* Five new genome types of adenovirus type 37 caused epidemic keratoconjunctivitis in Sapporo, Japan, for more than 10 years. *J Clin Microbiol* 2005;**43**:726–732.
10. Gordon YJ, Gordon RY, Romanowski E, Araullo-Cruz TP. Prolonged recovery of desiccated adenoviral serotypes 5, 8, and 19 from plastic and metal surfaces in vitro. *Ophthalmology* 1993;**100**:1835–1839 [discussion: 1839–1840].
11. Uchio E, Ishiko H, Aoki K, Ohno S. Adenovirus detected by polymerase chain reaction in multidose eyedrop bottles used by patients with adenoviral keratoconjunctivitis. *Am J Ophthalmol* 2002;**134**:618–619.
12. Okada M, Ogawa T, Kubonoya H, Yoshizumi H, Shinozaki K. Detection and sequence-based typing of human adenoviruses using sensitive universal primer sets for the hexon gene. *Arch Virol* 2007;**152**:1–9.